SPATIAL DISTRIBUTION OF GROUND SHAKING IN CHARACTERISTIC EARTHQUAKES ON THE WELLINGTON AND ALPINE FAULTS, NEW ZEALAND, ESTIMATED FROM A DISTRIBUTED-SOURCE MODEL

David J. Dowrick[1] and David A. Rhoades[2]

SUMMARY

A distributed-source model, recently developed by the authors, was used to study the spatial distribution of Modified Mercalli (MM) intensities and peak ground accelerations (PGA) in characteristic earthquakes, of M_w7.5 and 8.1 respectively, on the 75 km long Wellington fault and the 413 km long Alpine fault. In each event the predicted intensities reach MM10 and the PGAs reach 0.8g near the fault trace over much of its length, varying along it depending on the location of asperities. PGAs are related to MM intensity using a quadratic expression derived using New Zealand data. Comparisons are made between the PGA patterns estimated indirectly from the distributed-source MM intensity model and those estimated directly from a PGA model, which defines site-source distance as the shortest distance from the site to the fault. There are many similarities and some differences, the latter being attributable largely to the different methods of measuring site-to-source distances. Finally selected seismic risk issues for people and the built environment, including lifelines, are considered for Alpine fault earthquakes.

1 INTRODUCTION

In a recent study, Dowrick & Rhoades (2010) (D&R2010) developed a distributed-source model for estimating the spatial distribution of large crustal New Zealand earthquakes. The main purpose was to improve on the modelling of the inner Modified-Mercalli (MM) isoseismals of large shallow crustal earthquakes compared to that of the point-source models of Dowrick & Rhoades (1999; 2005a). An earlier informal attempt to address this problem has been made by Smith (2002), part of whose method was to put a patch on the along-strike attenuation function of the Dowrick & Rhoades (1999) model.

The model of D&R2010 gave a good fit to both the far-field and near-source isoseismal data of the 44 crustal earthquakes in their data set. In particular, the model fitted the near-source data of the largest earthquakes well.

In the present paper we apply the D&R2010 model to the problem of estimating the spatial distribution of Modified Mercalli intensities and peak ground accelerations (PGAs) in two large characteristic earthquakes in the New Zealand Seismic Hazard Model (NZSHM) (Stirling *et al*. 2007), ie earthquakes on the southern segments of (1) the Wellington fault and (2) the Alpine fault, with particular interest in near-source shaking. The locations of the surface traces of these two earthquake sources, as given by the NZSHM, are shown on Figure 1. The source parameters for the respective events, also from the NZSHM, are given in Table 1. The comparison of PGA estimates derived from MMI spatial distributions with those derived from direct modelling of instrumental strong-motion data is of much interest, because isoseismal determination involves subjective elements whereas instrumental recordings do not.

The risks arising from future earthquakes on these sources are appreciable. First, the Wellington fault runs through the capital city of New Zealand, and poses the highest seismic risk to both lives and property of any fault in the NZSHM. Second, the southern segment of the Alpine fault is notable because at 413 km long it is the longest active crustal fault segment in the country, expected to generate an earthquake of magnitude ~8.1, which is larger than every historical New Zealand earthquake except the 1855 Wairarapa earthquake of M_w 8.2. As its high intensities would occur in a zone of low population, it poses substantially less risk than the Wellington fault, but nevertheless is a dauntingly large event, and is of considerable scientific interest. Estimates of MM intensities and PGAs at selected population centres and key infrastructure sites are presented.

2 SOURCE MODELLING

To generate the isoseismals for the events under consideration using the D&R2010 model, we apply the source parameter data from Table 1 using the 2-D option of the geometrical configuration shown schematically on Figure 2. These source parameters are those in the current (2009) New Zealand Seismic Hazard model (The Alpine-fault data are published in Stirling *et al.* (2007) and the Wellington-fault data are from M. Stirling, pers. comm., 2009).

1 *Tauranga (Life Member)*

2 *GNS Science, Lower Hutt (Member)*

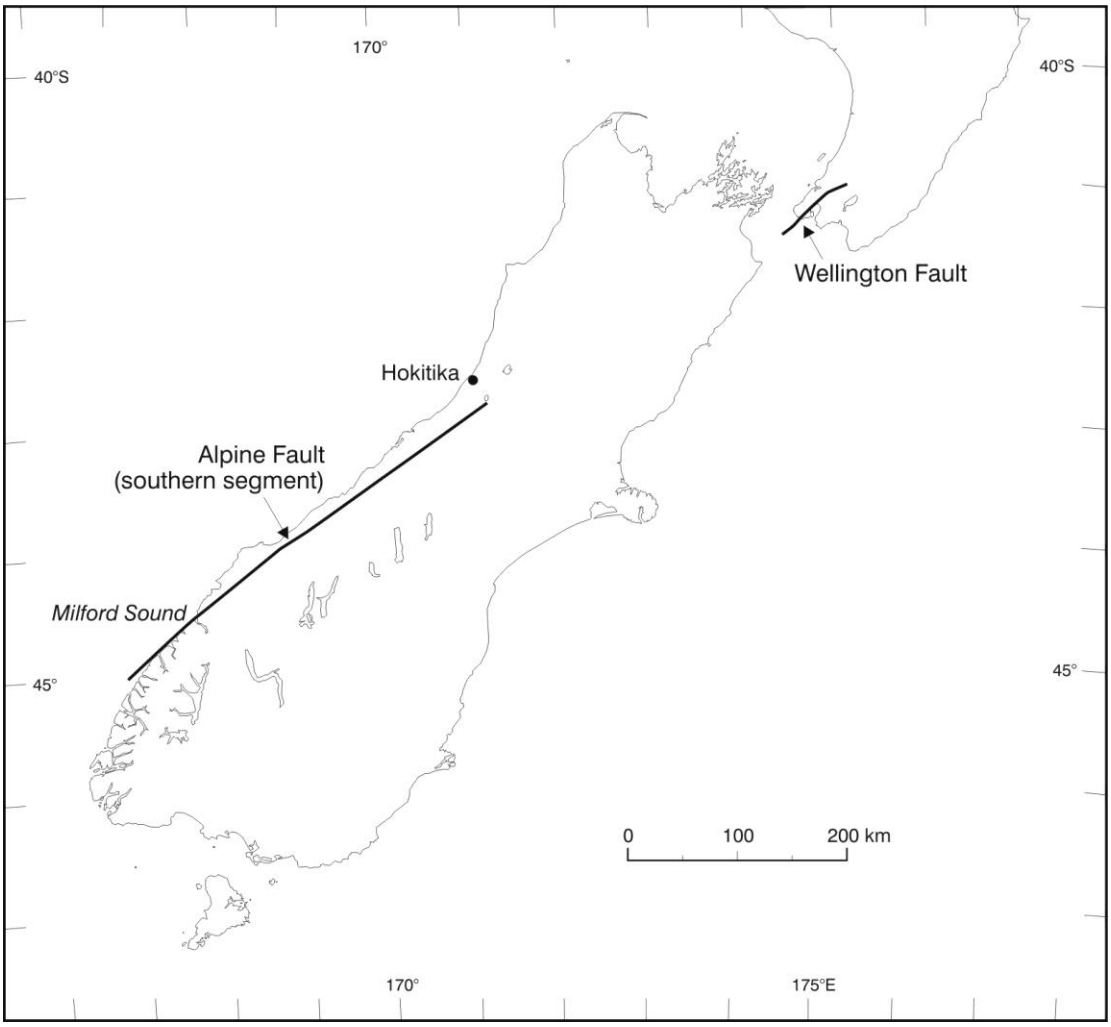

Figure 1: ***Map of New Zealand showing the locations of the sources of characteristic earthquakes on the southern segments of the Wellington fault and the Alpine fault.***

Table 1: Source parameters for the two characteristic New Zealand crustal earthquakes considered in this study (adopted from the 2010 version of the NZ Seismic Hazard Model).

Earthquake	h_t	M_w	Focal mech.	β	L (km)	W (km)	D (m)	D_a (m)	D_b (m)
Wellington fault	0	7.54	S	80	75	20	5.0	9.2	3.9
Alpine fault	0	8.06	S	60	413	13.9	8.0	14.6	6.2

Notes: h_t = depth to top of fault; β = dip; L = fault length; W = fault width; D = mean fault displacement; D_a = asperity displacement; D_b = non-asperity displacement.

In the absence of any present knowledge of asperities on these faults, we model possible asperities representative of Californian data from Somerville *et al.* (1999), as adapted in D&R2010. It is assumed that on an asperity the displacement takes a value D_a, and otherwise it takes the value D_b, and that D is the average displacement over the whole rupture surface. These data are plotted graphically on Figure 2, in terms of the normalised asperity area $A_{ar} = A_a / A$, the normalised asperity displacement $D_{ar} = D_a / D$ and the normalised non-asperity displacement $D_{br} = D_b / D$. Summing the moments on the asperities and non-asperities on the rupture surface, it can be shown show that

$$A_{ar}D_{ar} + A_{br}D_{br} = 1 \quad (1)$$

where the area of non-asperities A_b is given by

$$A_b = A - A_a \quad (2)$$

As in D&R2010 we adopt a value of D_{ar} = 1.83, and A_{ar}. = 0.21. It then follows from equation (1) that D_{br} = 0.78.

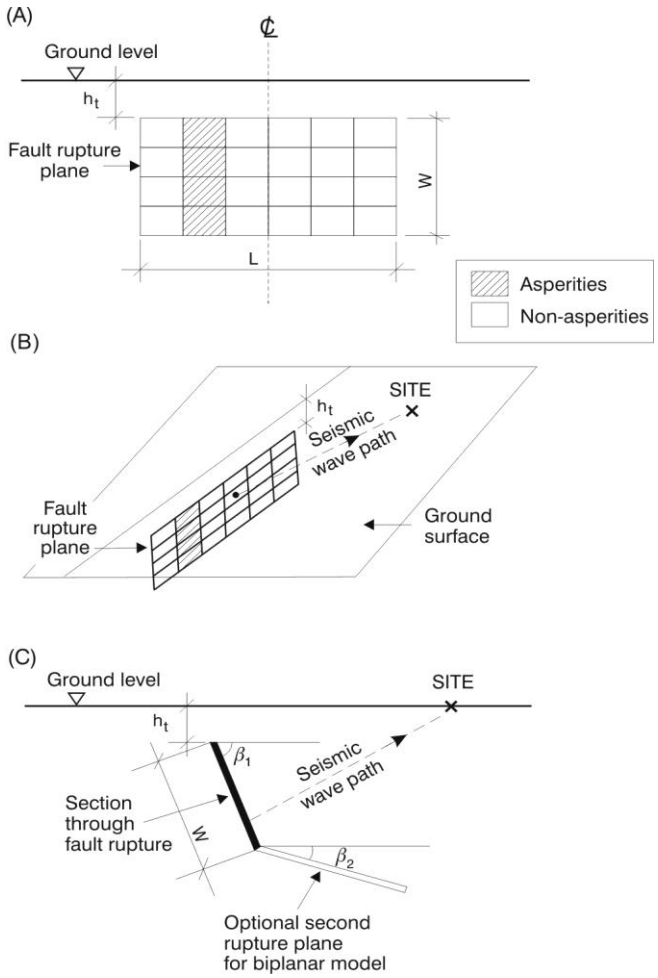

Figure 2: Simplified geometry of the fault rupture model, with asperities, as a 2-D or biplanar source, and its relationship to any chosen site on the ground surface (from Dowrick & Rhoades, 2010).

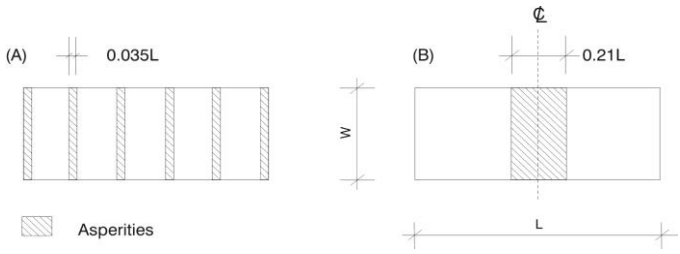

Figure 3: Distributions of asperities considered in the analyses where the area of asperities was 0.21 of the rupture area: (A) evenly spaced asperities, and (B) central asperities.

3 ISOSEISMALS OF A CHARACTERISTIC WELLINGTON FAULT EARTHQUAKE

The trace of the Wellington fault is not linear over its 75 km length. Therefore, in using our planar-source model, the top of the modelled source must be located so as to approximately match the actual fault trace. Here the location is chosen to maximise the estimated losses. Hence the trace of the model is made to coincide with the actual trace over its approximately linear sector (in the heavily built-up area) located between Thorndon in central Wellington and a point close to the junction of the Hutt and Whakatikei Rivers, Upper Hutt. The maximum distances between the actual trace and that of the model are 3 km at the northern end of the fault and 4 km at a location in Cook Straight 10 km from its southern end. A third of the length of the fault is offshore, where the location of the modelled near-source shaking is of little consequence from a risk point of view (except possibly from landslide-generated tsunami)

Figure 4 shows isoseismals estimated for the Wellington-fault earthquake when adopting the source parameters given in Table 1 and the asperity properties noted beneath equation (2). We consider both evenly spaced asperities (Figure 3A) and centrally located asperities (Figure 3B). The isoseismals estimated by the 2-D source model for these two sets of source and asperity properties are shown on Figure 4A and 4B respectively. Here it is seen that the two asperity distributions cause different spatial distributions of MM9 and MM10, but these differences are small. Of greater importance are the substantial differences between the shapes and lengths of the inner (MM9 and MM10) isoseismals predicted by the new models and those of Dowrick & Rhoades (2005a) (D&R2005a). The innermost isoseismals of the new models are longer and narrower than those of the 2005 model. In the case where asperities are located at the ends of the rupture (Figure 4A and 5Aa), the MM10 isoseismal is the same length as the fault rupture, and when there are no asperities near its ends (Figures 4B and 5Ba) the MM10 isoseismal is 2 km shorter than the rupture.

The attenuation graphs in the along-strike and strike-normal directions (*a* and *b*, respectively) corresponding to the 2-D source model and the D&R2005a model on Figure 4A are plotted on Figures 5A and 5B respectively. On the along-strike attenuation plots, it is seen that the intensity is MM10.1 over most of the length of the fault rupture when the asperities are evenly spaced (Figure 5Aa), and reaches MM10.2 along c. 40 percent of the length of the fault trace where the asperities are centrally located (Figure 5Ba). It is seen on Figures 5Aa and 5Ba that the attenuation curve estimated by the 2-D source model beyond the end of the fault exhibits reverse curvature: the physical necessity for this was explained in D&R2010. On the strike-normal plots, the attenuation curves for both the up-dip and down-dip directions are shown, as is the location of the horizontal projection of the rupture (W_h = 3.5 km) associated with the dip of 80º.

Smith (2002) also proposed an isoseismal model for a Wellington-fault earthquake, adopting a magnitude of M_w 7.34 and a rupture length of 68 km, and featuring a randomly located MM10 isoseismal as shown on Figure 6A.

The isoseismal model of Smith (2002) (Figure 6A) and that of the present study (Figure 4B) are rather different. For convenience of comparison, these two maps are overlain on Figure 6B. Here it is seen that the isoseismals of the D&R2010 model are both longer and wider than those of Smith (2002). This difference may be
partly due to the fact that the magnitude and fault length adopted by Smith are a little less than those in Table 1.

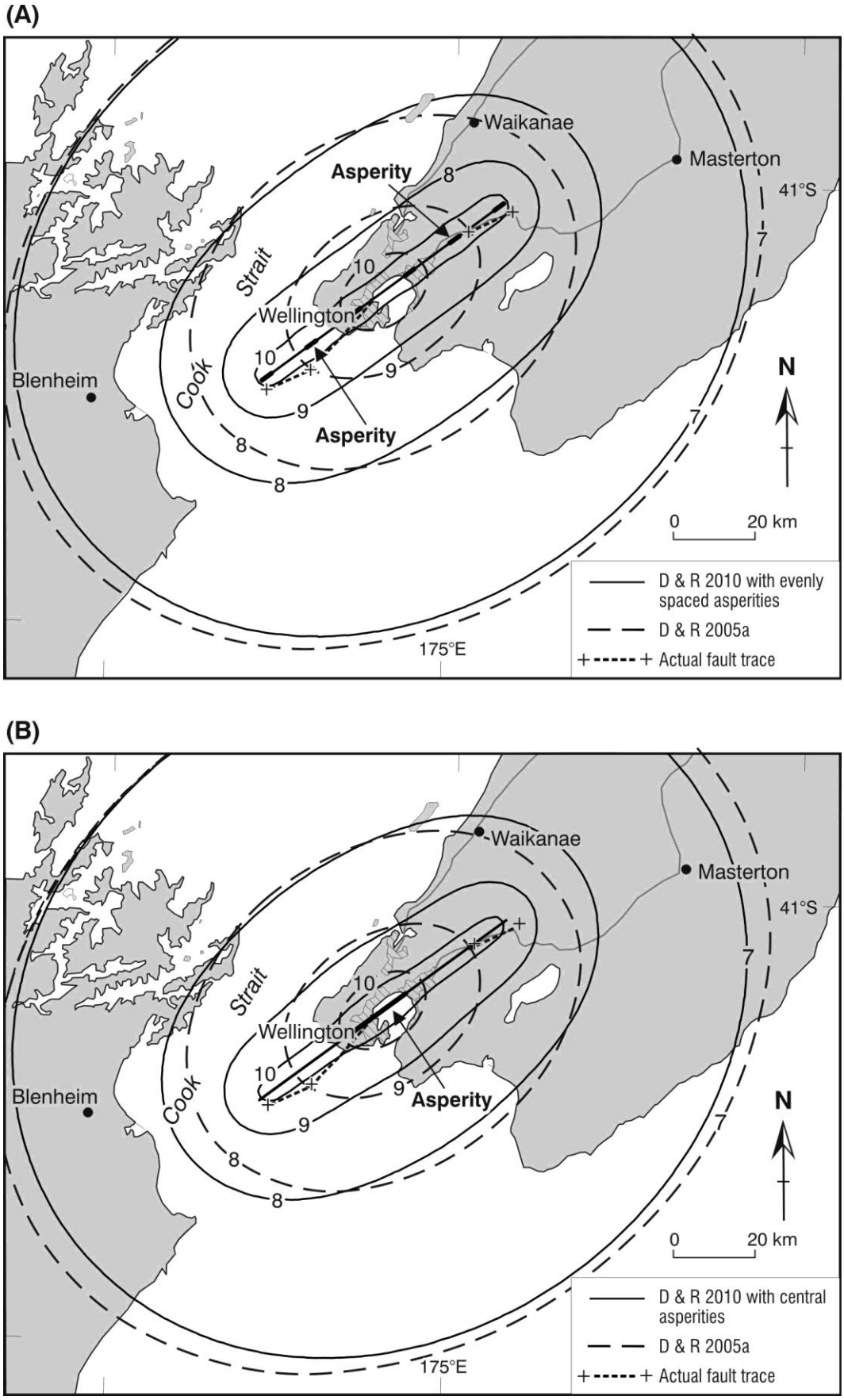

Figure 4: ***Maps of the inner isoseismals of a characteristic earthquake on the Wellington fault, using the Dowrick & Rhoades (2010) distributed-source model with: M_w = 7.54, L = 75 km, W = 20 km, D = 5.0 m, dip = 80° (northwest), h_t = 0, A_{ar} = 0.21: (A) evenly distributed asperities, and (B) central asperities. The isoseismals estimated by the model of Dowrick & Rhoades (2005a) are also shown.***

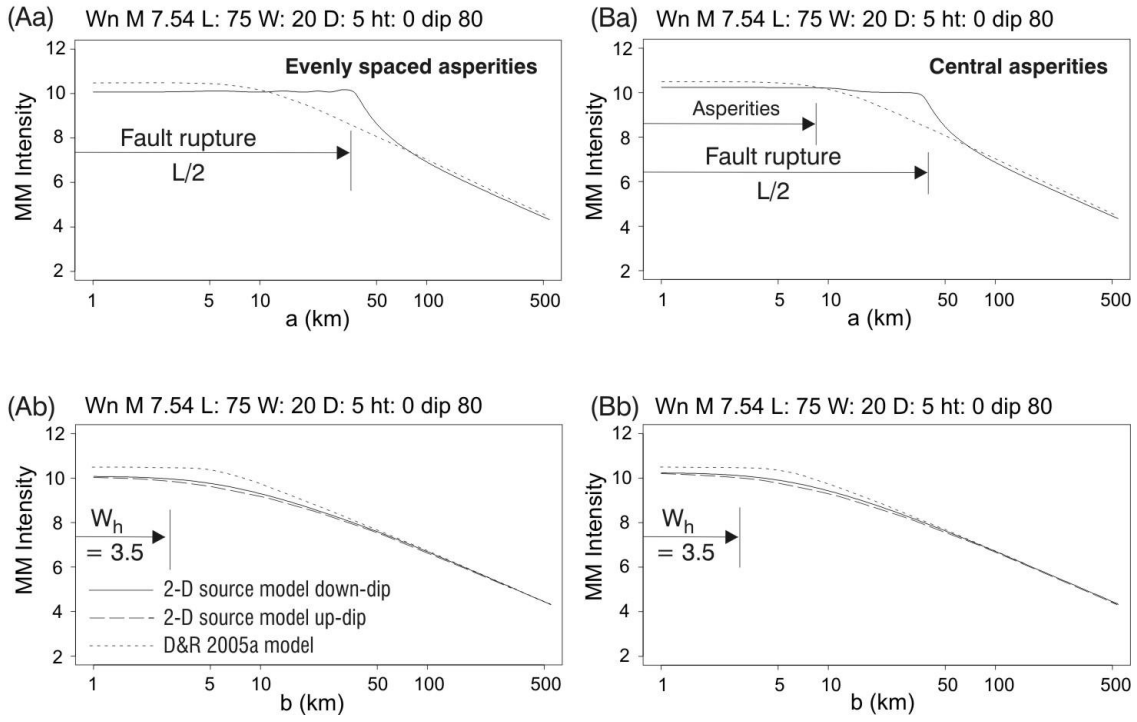

Figure 5: ***Attenuation plots in the along-strike direction a and the strike-normal direction b for the Wellington earthquake corresponding to Figure 4 for: (A) evenly distributed asperities, and (B) central asperities. The attenuation plots estimated by the Dowrick & Rhoades (2005a) model are also shown.***

4 ISOPGAS FOR THE WELLINGTON FAULT EARTHQUAKE

For using the 2-D source model for estimation of isoPGAs (PGA = peak ground acceleration) it is necessary to convert the isoseismals (eg those of Figure 4) to PGAs. Two relations for doing this are now considered, the first being that between MM isoseismals, I_{isos}, and PGAs for New Zealand earthquakes of Davenport (2003). This relation and the data from which it was derived are shown on Figure 7A. In the absence of a wider range of data, the log-linear portion of this relation is valid for isoseismals in the range $4 \le I_{isos} \le 7$ and is expressed by the equation

$$\log \mathrm{PGA} = -3.69 + 0.426 I_{isos} \quad s = 0.29 \qquad (3)$$

where PGA is in units of g.

Because the majority of the strong-motion-recording sites involved in the data set used by Davenport (2003) are located on firm ground, the above relation is considered to represent the mean response of Ground Class C as defined in the New Zealand Loadings Standard NZS 1170.5 (2004).

The second relation between MMI and PGA that we consider is of quadratic form, and arises as follows. Various studies (eg D&R2010) suggest that MM intensity in very large earthquakes appears to plateau at about MM10.5, and a PGA of 0.84g is within the scatter of worldwide recorded PGAs and is the median value of PGA estimated by the model of McVerry *et al.* (2006) for shallow soils at the fault trace of M7.5 reverse mechanism crustal earthquakes (see Figure 16 of McVerry *et al*., 2006). The McVerry *et al.* model is derived using overseas near-source PGA data recorded in large earthquakes. Therefore to relate isoseismals to PGA beyond the validity of the Davenport relation, ie for isoseismals > MM7, allowing for the saturation of both intensity and PGA, we have adopted a value of PGA = 0.84g at MM10.5. We have then fitted a quadratic expression to the Davenport relation for intensities MM4-MM7 and the point MM10.5 = PGA 0.84g. The resulting quadratic relation is given in equation (4) below:

$$\log \mathrm{PGA(g)} = -4.68 + 0.804 I_{Isos} - 0.0348 I_{Isos}^2 \qquad (4)$$

The Davenport and quadratic relations of equations (3) and (4) are plotted for comparison on Figure 7B.

Let us make a comment on uncertainties. The D&R model is derived from 267 (isoseismal distance, intensity) pairs from 44 earthquakes. The standard error of individual data points from the mean estimates of MMI in the D&R2010 model is 0.45 intensity units. However the standard error of the mean relation for is much smaller – about 0.03 units. Likewise, in the PGA model of McVerry *et al*. (2006), the total residual standard error for individual log PGA data points is 0.56. However, because again hundreds of individual points are used to determine the model, the standard error of the mean relation is much smaller – less than 0.05. This corresponds to a standard error of less than 12% on the median PGA estimate. Therefore the median value of 0.84g at the source of M7.5 crustal earthquakes in the PGA model has a standard error of less than 0.1. It follows that the quadratic relation (4) is similarly tightly constrained. These relatively small uncertainties on the mean modelled MM intensities and median modelled PGAs should be borne in mind when comparing PGA patterns below derived by two different procedures. While it is true that individual data points in the model and in future earthquakes will vary appreciably from the median relations, it is the median estimates that are considered here, and they are quite tightly constrained.

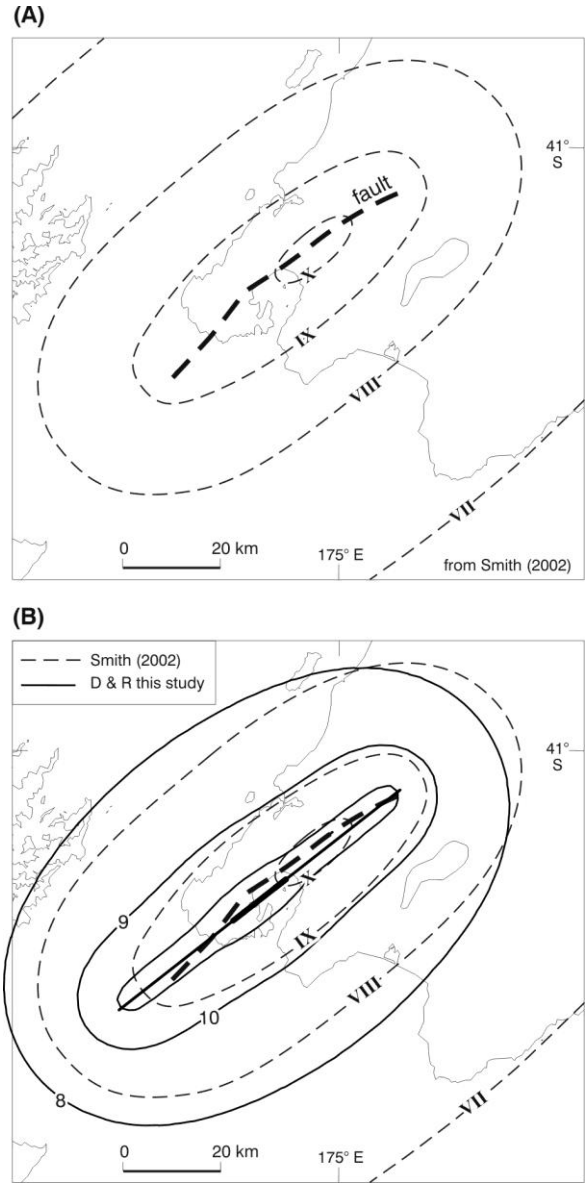

Figure 6: (A) Isoseismal map of an earthquake of M_w 7.34 on the Wellington fault proposed by Smith (2002), in which the MM10 isoseismal is due to randomly located asperities, and (B) Comparison of Figure 4B isoseismals for the Wellington fault earthquake from the D&R2010 model (with M_w 7.54 and centrally located asperities) with the isoseismals from Smith (2002) (with M_w 7.34) as shown on Figure 6A above.

Next we consider the spatial distribution of PGAs estimated for the Wellington-fault earthquake using the model of McVerry *et al.* (2006) assuming the values of M_w , L and h_t from Table 1 and a strike-slip-fault mechanism. The resulting isoPGA map is shown on Figure 9. Here the maximum estimated PGA at the fault trace is 0.78g, similar to the value of 0.81g found for Figure 8. It is seen that the overall patterns of spatial distributions of PGA are broadly similar on Figures 8 and 9, the differences between them resulting from the different ways in which the strength of shaking at any given site is calculated. In the McVerry *et al*. (2006) model, PGA is calculated using the shortest distance from the site to the source, so that on Figure 9 the isoPGA lines are constrained to be race-track shaped and to enclose the whole length of the fault. In the D&R2010 model, the MM intensity/PGA is calculated by combining the contributions from seismic moment radiated from all parts of the rupture surface, and the iso PGA lines are not constrained to enclose the fault. For example, on Figure 8 the line for PGA = 0.8g is 7 km shorter than the fault-rupture length of 75 km. In the case where asperities are located at each end of the fault rupture, the MM10 isoseismal is the same length as the rupture (see Figure 4A). Further, considering the case where the asperities are centrally located, as for Figure 4B, the intensity is in excess of MM10.2 over the central 20 km or so of the rupture (Figure 5Ba). Thus an isoseismal for MM10.2 (ie PGA 0.8g) would be about 20 km long, which is far shorter than the 75 km length of the rupture.

In the middle distance, the constrained race-track shapes of the isoPGAs of Figure 9 also differ somewhat from the isoPGAs of Figure 8. For example, on these two maps the areas inside the iso-lines for PGA = 0.3g are nearly equal, but the length/width ratio of the isoPGA line is 1.5 on Figure 8, and is 2.0 on Figure 9. Thus PGAs estimated by the McVerry *et al*. (2006) model at points in the hatched zones at the ends of the fault rupture (see Figure 9) are greater than those estimated for the same zones by the D&R2010 model of Figure 8. Considering three locations in the hatched zones, namely Levin, Featherston and Blenheim (see Figure 9), the PGA estimates from the McVerry *et al*. (2006) model, as shown on Table 2, are 18, 12 and 16 percent greater respectively than the corresponding estimates from the D&R2010 model. In contrast, at two locations outside of the hatched zones, ie Kapiti Island and Cape Palliser, the PGAs from the McVerry *et al*. model are only slightly greater than the PGAs from the D&R2010 model (as shown on Table 2).

Note that the slight asymmetry of the two hatched zones on Figure 9 arises from the slight asymmetry of the isoPGA line on Figure 8 caused by modelling the dip (80º) of the fault.

For ease of comparison, attenuation curves for the two models are plotted in the along-strike and strike-normal directions on Figure 10A and 10B. It is seen that in the along-strike direction, the D&R2010 model estimates lower PGAs than the McVerry *et al.* (2006) model from the end of the fault, out to a distance of 230 km. The greatest disparity is 27 percent at about a = 100 km.

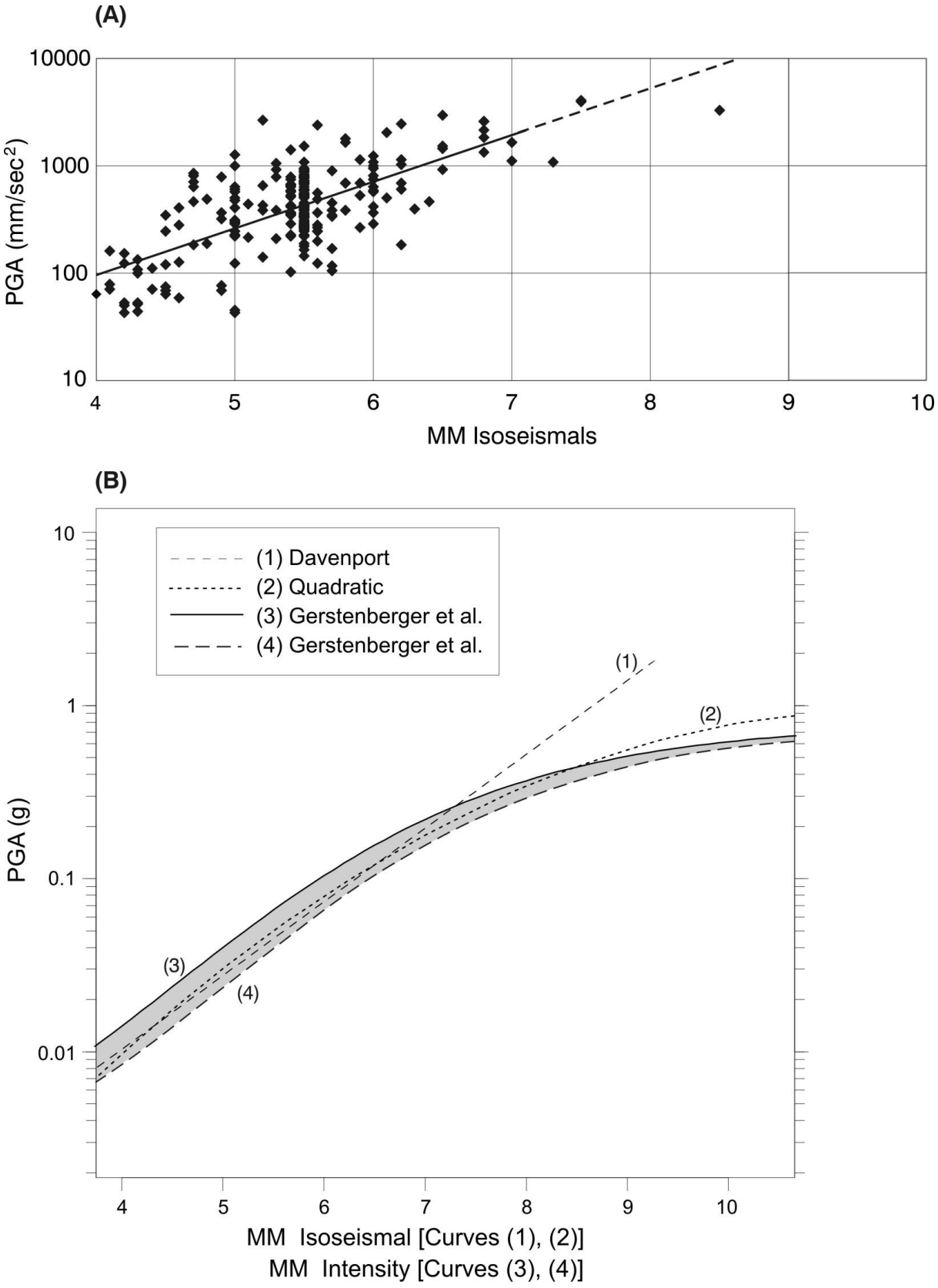

Figure 7: ***PGA vs. MM intensities (A) New Zealand data and relation of Davenport (2003) and (B) comparison of three PGA vs. MMI intensities relations from (1) Davenport., (2) quadratic modification of Davenport.***

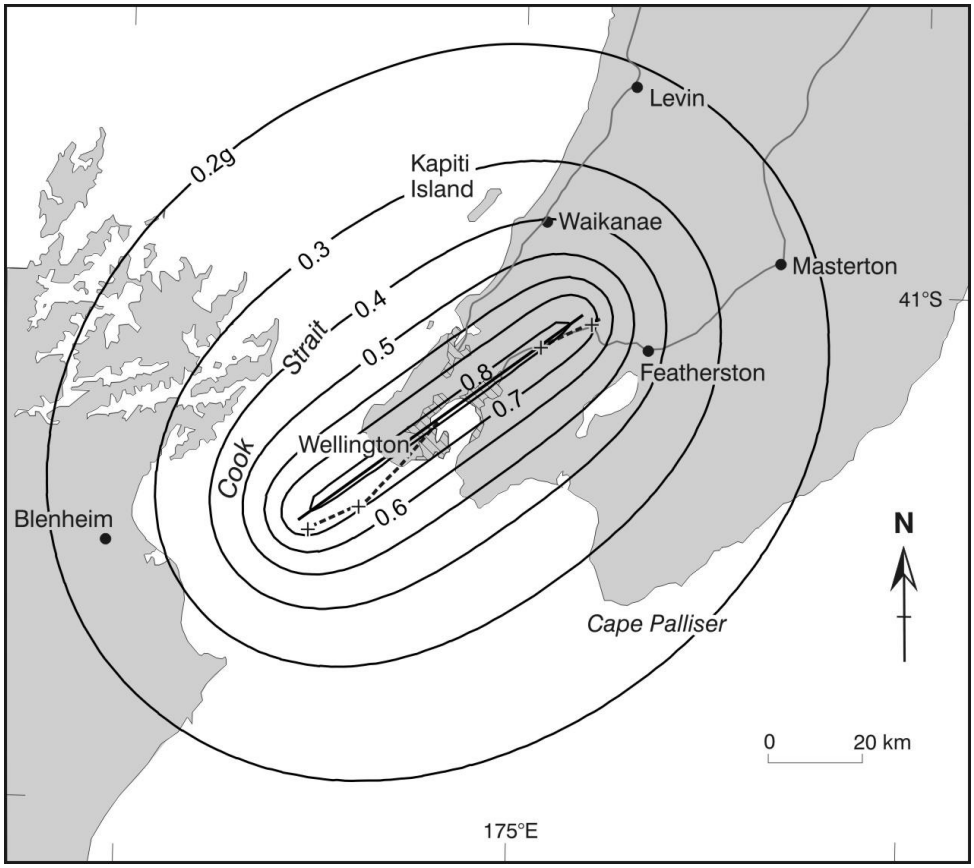

Figure 8: ***IsoPGA maps corresponding to Figure 4A except that the rupture is modelled without asperities, finding PGAs from New Zealand PGA vs. MMI quadratic relation quadratic (Figure 7B (2)).***

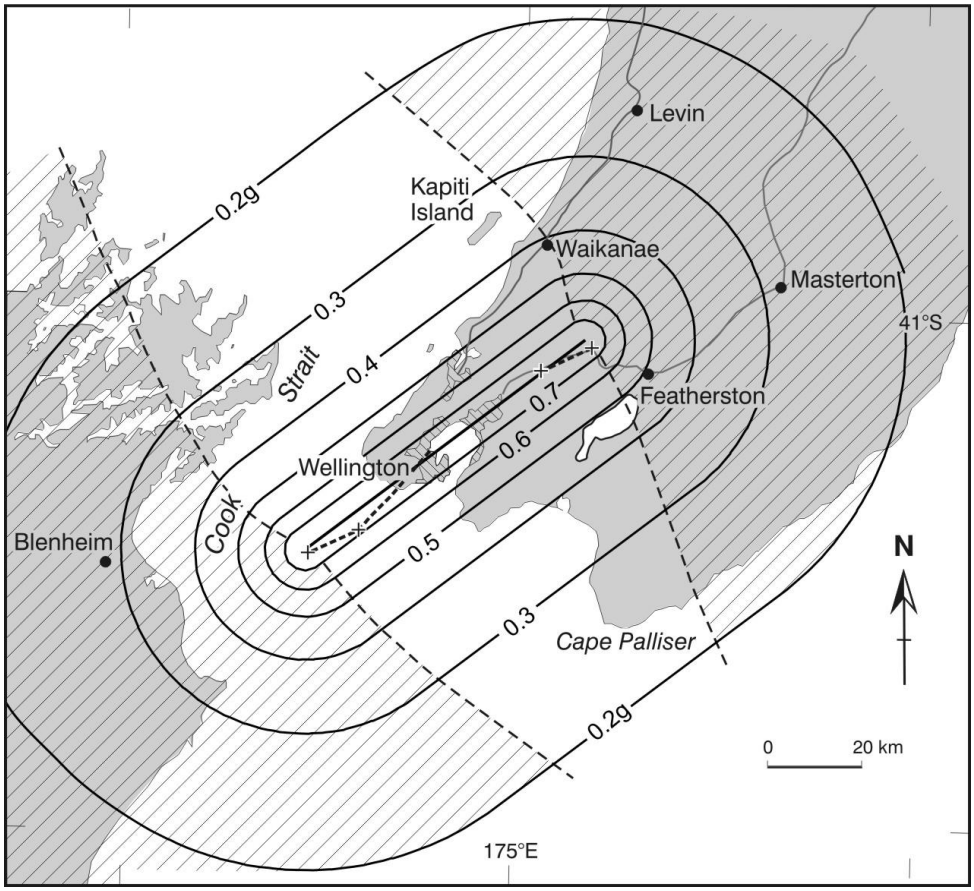

Figure 9: ***IsoPGAs for the Wellington fault earthquake (Figure 1) using the shortest-distance-from-source model of McVerry et al. (2006) for New Zealand Ground Class C. (The small effect of the fault dip has not been modelled.)***

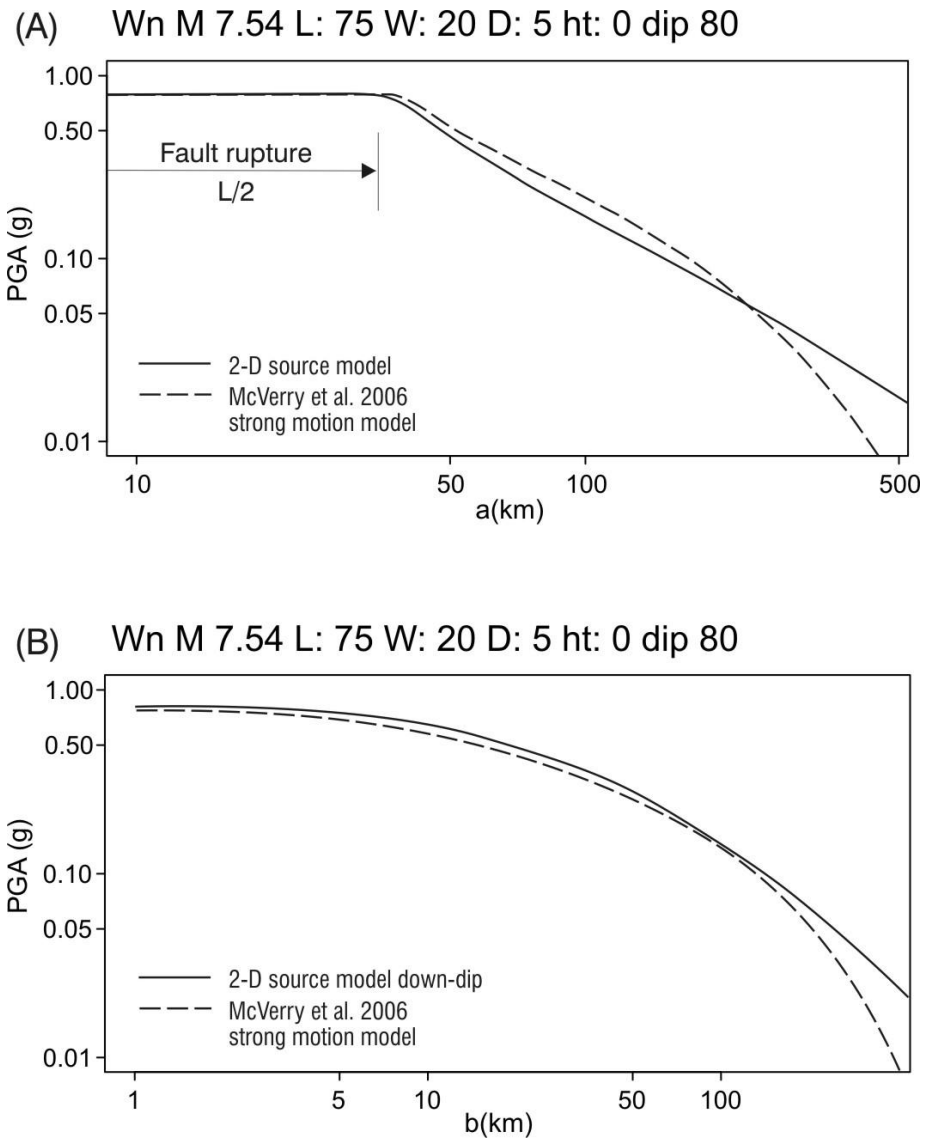

Figure 10: Attenuation plots of PGAs for NZ Ground Class C estimated for the Wellington fault earthquake corresponding to Figures 8 and 9: (A) along-strike (direction a) and (B) strike-normal (direction b, down-dip, north-west).

Table 2: Comparison of PGAs estimated at selected locations in a characteristic Wellington fault earthquake, as modelled on Figures 8 and 9.

Location	r_h (km)	**PGA8**(g) from Fig 8	**PGA9**(g) from Fig 9	**PGA9/PGA8**
Levin	25	0.22	0.26	1.18
Featherston	8	0.48	0.54	1.12
Blenheim	21	0.25	0.29	1.16
Kapiti Island	15	0.35	0.34	0.97
Cape Palliser	27	0.26	0.25	0.96

Note: r_h is the shortest distance from the site to the fault trace.

5 ISOSEISMALS OF A CHARACTERISTIC ALPINE-FAULT EARTHQUAKE

We next consider the isoseismals estimated for a characteristic earthquake on the southern segment of the Alpine fault when adopting the source parameters given in Table 1, and the asperity properties noted beneath equation (2). Here we consider only the case where the asperities are located at the centre of the fault rupture (as on Figure 3B). The isoseismals estimated by the D&R2010 model are shown on Figure 11A.

The attenuation of intensity in the along-strike and strike-normal directions (*a* and *b*) are plotted on Figures 12A and 12B respectively. These figures show that the maximum intensity at the centre of the fault trace is I_0 = MM10.3, which is virtually the same as the value of I_0 = MM10.2 estimated for the characteristic Wellington fault earthquake (Figures 4 and 5).

As seen on Figure 11A, the intensity reaches MM10 close to the fault trace and the MM10 isoseismal just fails to enclose the full length of the fault rupture. Because of the narrowness of the innermost isoseismal, this is easier to see on Figure 12. For example, Figure 12B shows that the MM10 isoseismal is 10 km wide at the centre of the fault trace, where the asperities are clustered. The central zone of asperities is 43 km long, so that at a distance of about 25 km from the mid point of the rupture, we found (in a plot not shown here) that the width of the MM10 isoseismal reduces to 7 km along the rest of the fault rupture.

A different approach is adopted for locating the isoseismals from that used above for the Wellington fault event. As seen on Figure 1, the line of the Alpine fault deviates by up to about 12 km from a straight line over its 413 km length. Therefore, rather than overlaying the model of Figure 11A on an approximate median location of the fault trace, we have manually curved the isoseismals so that the location of the fault trace of the model approximately fits the shape of the actual fault trace, as shown on Figure 11B. In view of the slightness of the curvature of the fault trace, this procedure is judged to provide a satisfactory model of the spatial distribution of the intensities for this event. In any case, the southern segment of the Alpine fault (Figure 1) passes through a largely unpopulated mountainous region, and hence the exact location assumed for the trace of the modelled fault rupture has little effect on losses estimated using the modelled intensities.

In the data set used to develop the D&R2010 model, the longest fault rupture was 145 km, which is substantially less than the 413 km length of the Alpine-fault segment modelled in Figure 11. To examine the validity of this extrapolation, we plotted the attenuation in the along-strike direction for four fragments of the fault (assuming no asperities), comprising earthquakes having the same values for the source parameters W, D, h_t and dip, but a range of lengths L = 30, 50, 200 and 413 km and consequent magnitudes in the range 7.30 to 8.06. Four attenuation plots are shown on Figure 13. Here it is seen that the estimated intensity along the fault trace has saturated at MM10.3 when L = 30 km, and is constant for all greater rupture lengths. Thus the maximum MM intensity in the D&R2010 model is stable for earthquakes with very long ruptures.

In addition to modelling the Wellington-fault earthquake (Figure 6A), Smith (2002) proposed the isoseismal map for the Alpine fault shown on Figure 14, based on a rupture length of 479 km and magnitude M_w 8.07. We note that neither the nature of the asperities nor the basis for estimating the MM10 isoseismal was explained in Smith (2002). The model on Figure 14 is broadly similar to the new map proposed on Figure 11B, in that the MM9 isoseismal encloses the full length of the fault rupture. However the two maps are somewhat different in detail:

1. Unlike Figure 11B, Figure 14 does not have an MM10 isoseismal that encloses the full length of the rupture.

2. The MM10 isoseismal in Figure 14 due to a randomly located asperity is 40 km long and 20 km wide, while that of Figure 11B is twice as long (86 km, ie $\approx$ the length of the asperity) and half as wide (10 km).

3. The MM9 isoseismal in Figure 14 is 48 km wide over its full length, while that of Figure 11B is 35 km wide at the middle of the asperity and 30 km wide away from the asperity. Thus the Smith (2002) MM9 isoseismal (unlike that of Figure 11B) does not show the influence of the asperity.

6 ISOPGAS FOR A CHARACTERISTIC ALPINE-FAULT EARTHQUAKE

Again we use the quadratic relation (equation (4)) to convert an isoseismal map to PGAs. We consider an Alpine-fault earthquake similar to that shown on Figure 11B – except that no asperities have been modelled (so that a direct comparison can be made with the McVerry *et al*. model). The resulting PGA map of the Alpine-fault earthquake is shown on Figure 15.

The spatial distribution of PGAs for the Alpine-fault earthquake estimated using the model of McVerry *et al.* (2006), assuming the values of M_w , L and h_t from Table 1 and a strike-slip-fault mechanism, is shown on Figure 16. Here the maximum PGA at the fault trace is 0.82g, which is essentially the same as the value of 0.83g found for Figure 15. It is seen that the overall patterns of spatial distributions of PGA are broadly similar on Figures 15 and 16, the differences between them resulting from the strong-motion-modelling assumption that the site-to-source distances are always the shortest distance between them. This means that on Figure 16 all the isoPGA lines are constrained to be race-track shaped, and the innermost one must enclose the top of the fault. On Figure 15, the line for PGA = 0.8g is about one kilometre shorter than the fault rupture length of 413 km.

18 sites of interest in the southern South Island are listed in Table 3, together with their distances (r_h) from the fault and the estimated MM intensities and PGAs on Figures 11B, 15 and 16. It is seen that the PGAs estimated by the two different methods are closely similar in all but four cases, ie Lake Coleridge, Manapouri, Otira Viaduct and Hokitika River Bridge. These sites are all in the hatched zones near the ends of the fault rupture (cf. Figure 9), with the McVerry *et al*. (2006) model (Figure 16) estimating PGAs 12-29 percent larger than those obtained using the D&R2010 model (Figure 15).

Outside of the hatched zones the discrepancies between the isoPGA shapes of the two models are apparent only near the east coast, eg at Oamaru (r_h =190km) the McVerry *et al*. (2006) and D&R2010 models estimate PGAs of c. 0.08g and c. 0.10g, respectively.

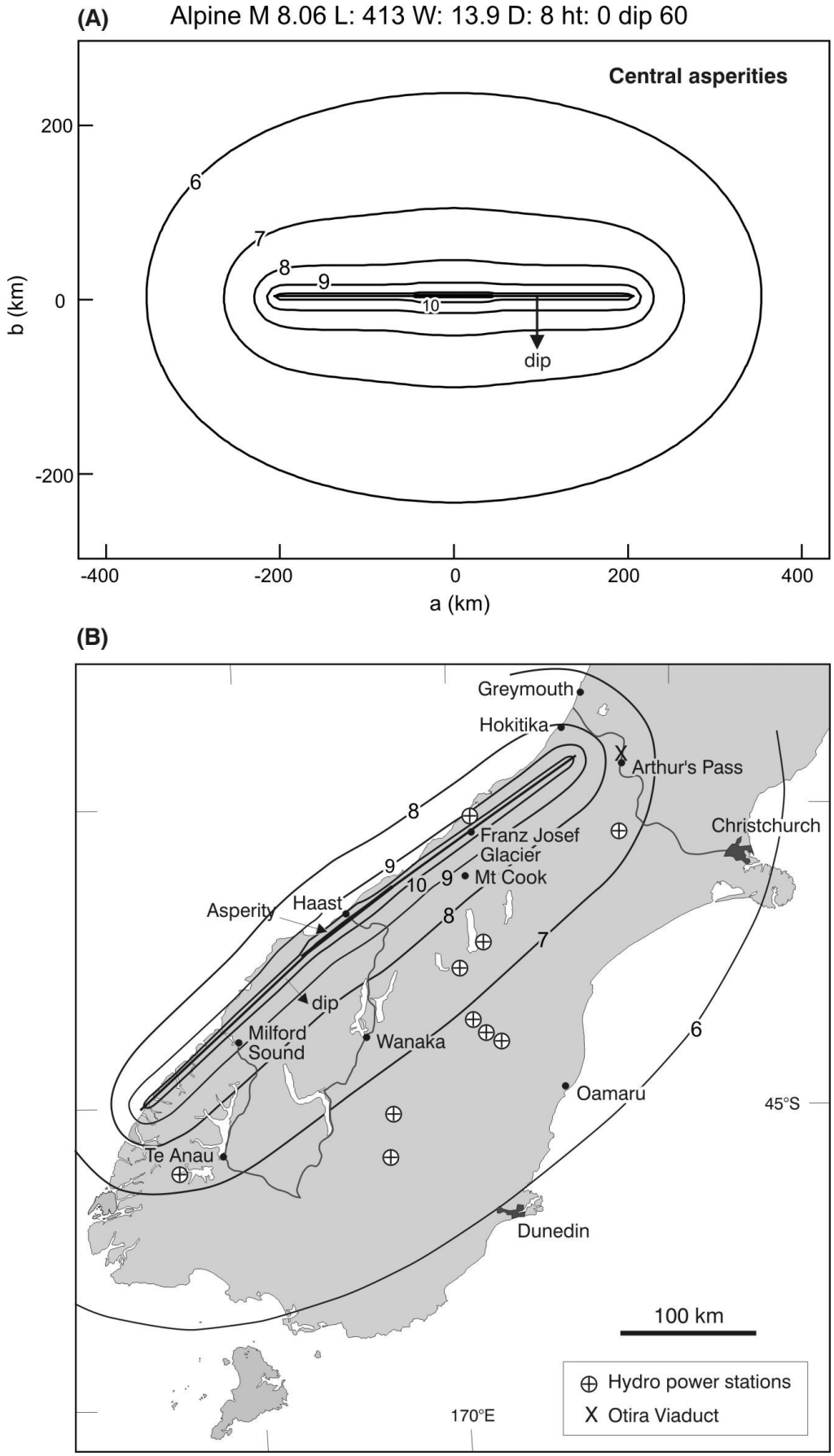

Figure 11: ***Isoseismal maps of a characteristic earthquake on the southern (Fiord-Kelly) segment of the Alpine fault using the D&R distributed-source model, assuming centrally located asperities, M_w = 8.06, L = 413 km, W = 13.9 km, D = 8 m, dip = 60° (southeast) and h_t = 0, (A) Map as produced by the software (ie with a linear fault trace), and (B) Map with the isoseismals from (A) curved by hand to follow the line of the fault.***

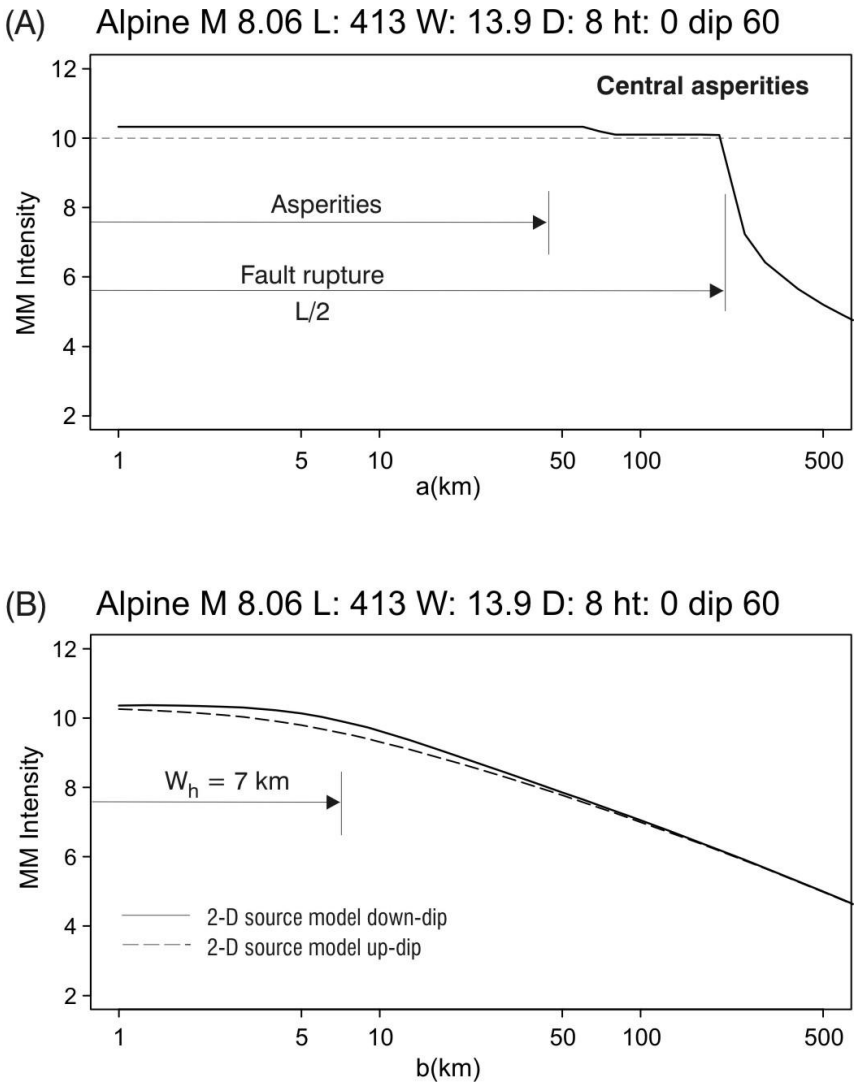

Figure 12: ***Attenuation plots for the Alpine fault earthquake, corresponding to Figure 11, (A) along-strike (direction a) and (B) strike-normal (direction b).***

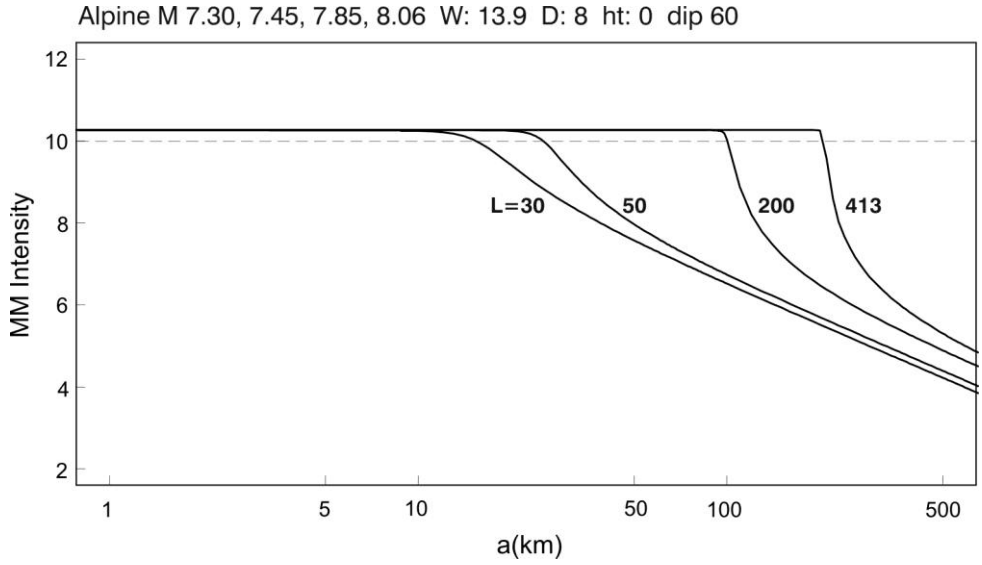

Figure 13: ***Attenuation plots in the a-direction of "fragments" of length L = 30, 50, 200 and 413 km of the southern segment of the Alpine fault, with no asperities, and W = 13.9 km. The magnitudes associated with the four fault fragments are M_w = 7.30, 7.45, 7.85 and 8.06, respectively.***

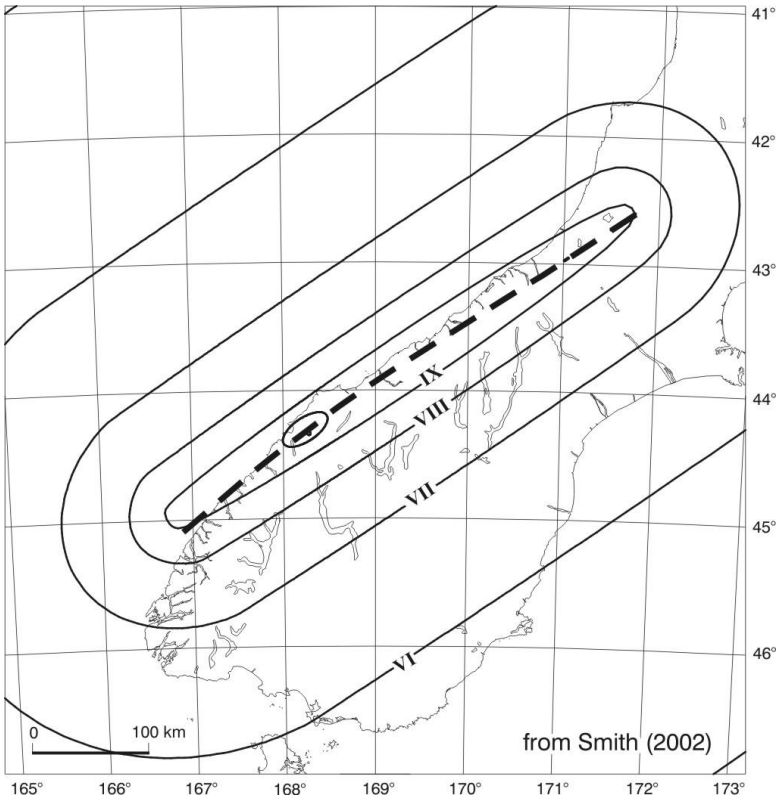

Figure 14: ***Isoseismal map of an Alpine fault earthquake of M_w = 8.07 proposed by Smith (2002), in which the MM10 isoseismal is due to randomly located asperities. Compare with the new map estimated using the model of D&R (2010) shown on Figure 11B.***

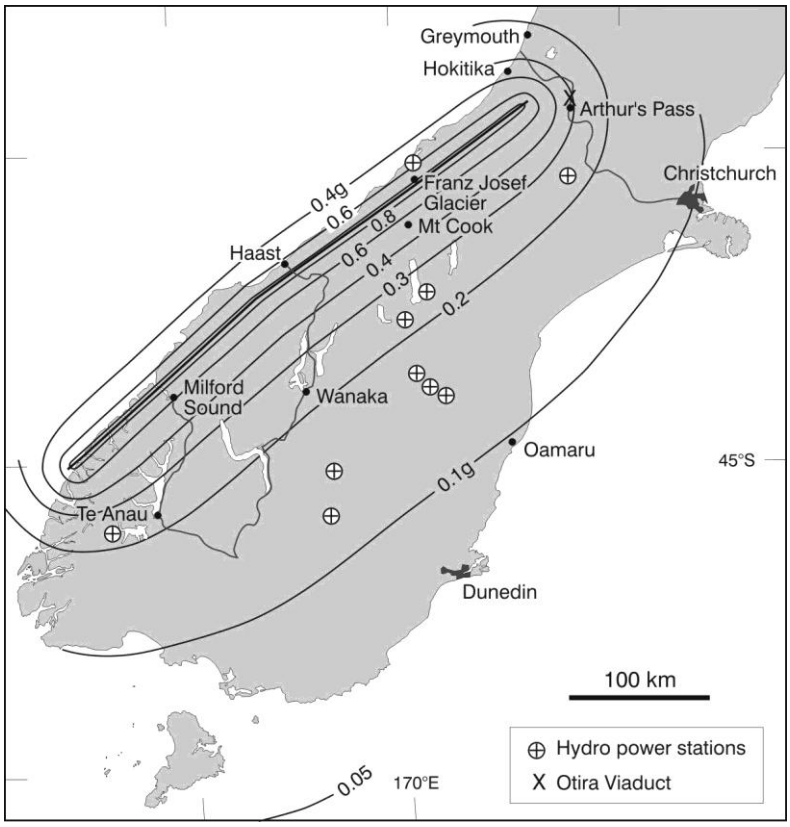

Figure 15: ***IsoPGA maps corresponding to Figure 11B except that the rupture is modelled without asperities, finding PGAs from New Zealand PGA vs. MMI quadratic relation (Figure 7B). The fault dips 60º southeast.***

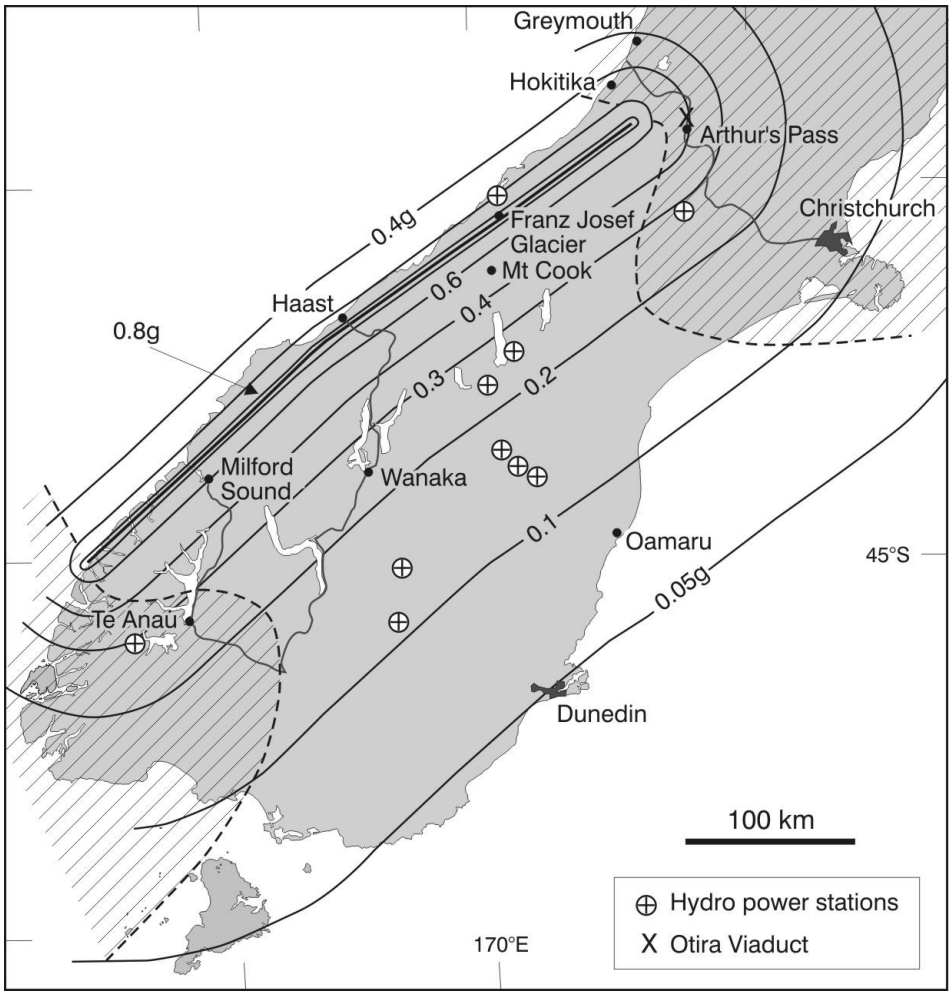

Figure 16: IsoPGAs for the Alpine fault earthquake (Figure 1) using the shortest-distance-from-source model of McVerry et al. (2006), for New Zealand Ground Class C. (The small effect of the fault dip has not been modelled.)

Table 3: MM Intensities and PGAs estimated for selected major lifelines sites and Mt Cook (listed from north to south) in the characteristic Alpine fault earthquake.

Location	r_h (km)	**MMI** from Fig 11B	**PGA**(g) from Fig 15	**PGA**(g) from Fig 16
Power Stations				
L Coleridge	65	7.3	0.25	0.28
L Wahapo	9	9.3	0.68	0.68
Tekapo A,B	72	7.4	0.24	0.25
Ohau A-C	76	7.4	0.23	0.24
Benmore	112	6.9	0.18	0.17
Aviemore	127	6.9	0.17	0.16
Waitaki	132	6.8	0.16	0.15
Clyde	126	6.8	0.16	0.15
Roxburgh	150	6.6	0.13	0.12
Manapouri	55	7.4	0.24	0.30
Road Structures				
Otira Viaduct	40	7.8	0.31	0.40
Hokitika R Bridge	24	8.3	0.40	0.46
Haast R Bridge	5	9.9	0.75	0.76
Homer Tunnel	23	8.7	0.50	0.50
Mountain Peak				
Mt Cook	19	8.8	0.55	0.55

Note: r_h is the shortest distance from the site to the fault trace.

Attenuation curves for the two models in the along-strike and strike-normal directions are plotted on Figure 17A and 17B. In the along-strike direction (Fig. 17A), the PGAs of the McVerry *et al*. (2006) model are higher from the end of the fault out to a distance of 450 km. The disparity is greatest at about a = 300 km, where the McVerry *et al*. (2006) PGA value is 54 percent larger than that of the D&R2010 model.

7 SOME SEISMIC-RISK IMPLICATIONS

The major seismic risk issues for the Wellington-fault earthquake are rightly much studied and will not be discussed here, except to note that in a recent study of casualties in a Wellington-fault earthquake, Cousins *et al.* (2008) estimate that in a daytime event there would be 600 deaths and 4400 hospitalised injured. We point out that studies based on the inner isoseismals estimated by the D&R1999 or D&R2005a or models may warrant review, using the heavily revised isoseismals of the distributed-source model presented here (eg see Figure 4B).

The very large characteristic earthquake on the Alpine fault has serious consequences for the 7000 or so West Coast residents living from about Hokitika southwards. As the southern segment of the Alpine fault ruptures on average at approximately 300 year intervals and last ruptured c. 1717 AD (Sutherland *et al*., 2007), its MM10 and MM9 zones represent the highest seismic hazard in New Zealand. The zone of shaking causing substantial damage is bounded approximately by the MM8 isoseismal, which lies c. 40 km southeast of the fault. Fortunately, as seen on Figure 11B, the zone extending 30 km or so eastwards of the MM10 isoseismal is a largely uninhabited mountainous area. Thus there will be generally only light consequences for residential localities east of the Southern Alps. A brief discussion of some of the seismic risk considerations is given below.

On the new isoseismal map of the Alpine-fault earthquake (Figure 11B), the PGA map derived from it (Figure 15), and the PGA map derived from the model of McVerry *et al.* (2006) (Figure 16) are plotted the locations of:

- the main urban areas (all small) within the MM8 - MM10 zones,
- the main roads within the MM7-10 zones,
- 13 hydro-electric power stations situated south of Greymouth, and
- the Otira Viaduct, the Hokitika River bridge, the Haast River bridge and the Homer Tunnel.

The populations given below are derived from the 2006 Census. Consider first the residents of the zone of strongest shaking, ie the intensity **MM10 zone** (inside the MM10 isoseismal)**,** containing a little upwards of 1,040 residents. Considering urban areas of 100-or-more residents, the four largest settlements are Whataroa, Franz Josef Glacier, and Fox Glacier, comprising 575 people. The **MM9 zone** had a little upwards of 1,640 residents, of whom 630 were in Kokotahi, Kowhitirangi, Waitaha, Harihari and Milford Sound. The **MM8 zone** had a little upwards of 4,750 residents, of whom 4,083 were in Kaihinu, Arahura, Hokitika (3,078), Takutai, Kaniere, Mananui and Mount Cook Hermitage. (In addition to residents, considerable numbers of tourists will also be at risk, depending on the time of year).

Virtually all houses in the MM10 zone are likely to be damaged, many seriously (Dowrick *et al.* 2001). Similar performance should be expected from non-domestic property, based on extrapolation from the damage in the MM9 zone of the 1987 Edgecumbe earthquake (Dowrick & Rhoades, 1993). Few casualties can be expected in or near houses, particularly those of timber construction, and this may apply to much of the MM10 non-domestic property (Dowrick & Rhoades, 2005b).

Danger to people in the MM8 - MM10 zones arises from the expected high incidence of landslides and avalanches in the steep mountain terrain (see the New Zealand MM intensity scale, Dowrick *et al*. (2008)). In the 1929 M_w 7.7 Buller (Murchison) earthquake, also centred in a mountainous area of sparse population, all of the16 deaths were caused (one indirectly) by landslides or rock falls (Dowrick, 1994). As seen in Table 3, New Zealand's highest mountain, Mount Cook (located on Figures 11, 15 and 16), is estimated to experience intensity of nearly MM9 and PGAs (on flat ground) of about 0.5 g. But strong amplification will occur in this steep peak, and the duration of strong shaking will be considerable, so substantial rock slides are to be expected here. Mount Cook lost 10 m of its lofty peak in a small slide in 1991 (M. McSaveney, pers. comm., 2009), in the absence of any ground shaking, so it will be interesting to observe how much height it will lose in very strong and prolonged earthquake shaking.

There are hundreds of mountain peaks and ridges in the 30,000 square kilometre MM8 - MM10 zone, where the flat-ground shaking will have horizontal PGAs in the approximate range 0.35 - 0.75g which will be subject to amplifications of 2 (or possibly substantially more). This means that unsecured people on stable but very strongly shaken sites are very likely to be thrown down, some down steep slopes. For example, two men working on the top of Mount Edgecumbe during the 1987 Edgecumbe earthquake were thrown to the ground (fortunately locally flat), which is consistent with topographical amplification (to MM8) of the flat ground intensity of MM7 around the base of the mountain. The threshold for difficulty in standing is at intensity MM7 (PGA ~0.2g).

Topographical amplification in steep peaks in very strong shaking has been observed, for example causing very large landslides on Mount Stanley in the 1929 Buller (Murchison) earthquake (Dowrick, 1994). But as the amount of topographical amplification in such strong shaking has not yet been instrumentally measured in the field, the recording of ground motions on the peak and at the base of a steep mountain peak near the fault in the next Alpine fault earthquake would be of considerable scientific interest. Two (of many) candidate mountains are Mt Mark and The Woolstack which are about 3 km from the Alpine fault and a few minutes by helicopter from Haast. They are both about 1500 m high and below the permanent snowline.

Seventeen major lifelines sites south of Hokitika, including four large road structures and all of the hydro-electric power stations, are located on Figures 11, 15 and 16, and are listed in Table 3. It is seen that the road structures would be subjected to moderate to very strong shaking in this earthquake, the long Haast River bridge being particularly strongly shaken. Just inland from this bridge the State Highway crosses the fault, so it will be completely dislocated by the 8m horizontal throw of the fault. The small Westland power station at Lake Wahapo is only 9 km from the fault and would be tested by very strong shaking, with estimated PGAs of 0.68g and an intensity of MM9.3. The other power stations range in distance from 55 to 150 km from the fault with correspondingly less strong shaking, the worst affected being Manapouri with estimated PGAs of 0.24g and 0.30g (depending on the predictive model).

It should be borne in mind that, because of the uncertainty in estimating individual PGAs for data points from models, the actual PGAs at any facility could be three times greater or three times less than the estimated values.

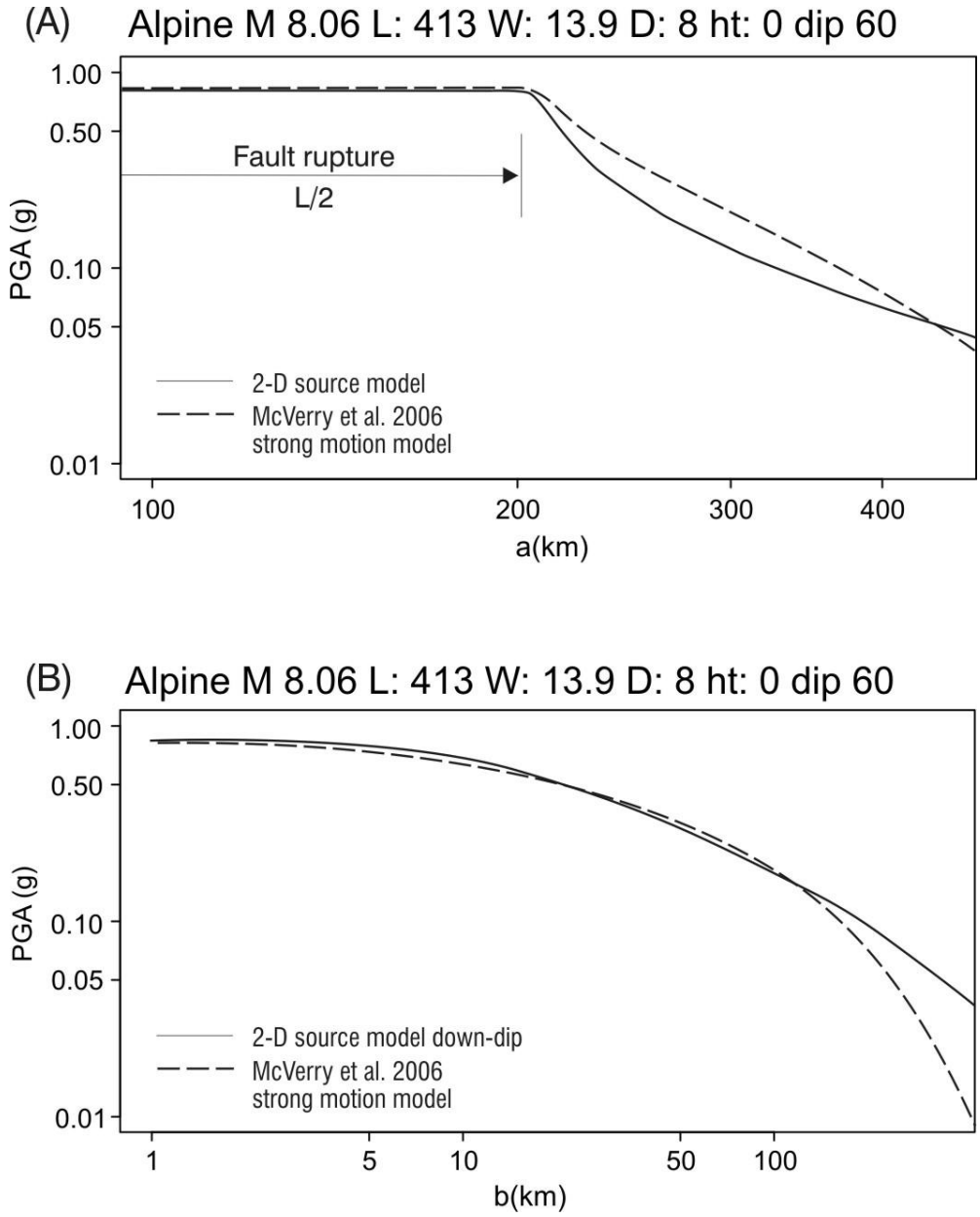

Figure 17: Attenuation plots of PGAs estimated for NZ Ground Class C for the Alpine fault earthquake corresponding to Figures 15 and 16: (A) along-strike (direction a) plotted from a = 100 km, and (B) strike-normal (direction b, down dip, south-east).

8 CONCLUSIONS

From the above study, the following conclusions have been drawn:

1. For a characteristic M_w 7.5 Wellington fault earthquake, the distributed-source model (D&R2010) estimates an MM10 isoseismal extending close to the full length of the fault rupture and 7-10 km wide, depending on the locations of asperities. This isoseismal is substantially longer and narrower than estimated by the earlier model of D&R2005a.

2. For a characteristic M_w 8.1 Alpine fault earthquake, the D&R2010 model estimates MM10 isoseismals the lengths of which are 100 and 98 percent of the rupture length respectively in the cases where (a) there are no asperities and (b) where asperities are clustered at the centre of the rupture. As for the Wellington earthquake, the estimated widths of the MM10 isoseismals for the Alpine event are 7-10 km depending on the asperities.

3. The maximum intensities estimated at the centre of the fault trace occur in the central asperities case, and are MM10.2 and MM10.3 for the Wellington-fault and Alpine-fault events respectively. The similarity of these values is due to the saturation of maximum intensity for faults longer than c. 30 km in the D&R2010 model.

4. A quadratic expression for predicting PGAs from MM isoseismals has been developed by fitting it to New Zealand data in the range MM4-MM7 and fixed at PGA = 0.84g when the intensity is MM10.5. The latter data point is shown to model near-source PGA's consistent with those of the McVerry *et al*. (2006) model (see next conclusion).

5. Comparisons have been made of the PGAs estimated for the Wellington-fault and Alpine-fault earthquakes using the strong-motion model of McVerry *et al*. (2006) and PGAs obtained by transforming the intensities estimated from the distributed-source model of D&R2010 using the quadratic relation mentioned above. Both approaches estimate near-fault mean PGAs of c. 0.8g for both events. The biggest differences between their estimates are in the semi-circular zones at the ends of the ruptures, where the isoPGAs are constrained by the McVerry *et al*. (2006) model to enclose the whole length of the fault. The McVerry *et al*. model PGA estimates are up to 54 percent higher than those derived from the D&R2010 model at sites in these zones.

6. Apart from differences attributable to the different treatments of source distance, the PGA estimates derived from the McVerry *et al* and D&R2010 models for theses two sources are rather similar.

7. From a national perspective, the seismic risk posed by the Alpine fault is low. However, for the small (7000) residential population plus the variable tourist population of the near-source areas, the damage to the built environment will be serious because intensities will reach MM10, while the casualties consequential to that damage are expected to be light.

8. People in the 30,000 km^2 mountainous region affected by intensities MM8 - MM10 will be at considerable risk from landslides, many worsened by topographical amplification.

9. As topographical amplification in steep peaks in very strong shaking has not yet been instrumentally measured in the field, the recording of ground motions on the peak (and at the base) of a steep mountain peak near the fault (eg Mt Mark) in the next Alpine fault earthquake would be of considerable scientific interest.

10. Of the selected lifelines considered here, the three most at risk are the Lake Wahapo hydro-electric power station (MM9.3), the Haast River bridge (MM9.9), and the Hokitika River bridge (MM8.3).

9 ACKNOWLEDGEMENTS

The authors thank Graeme McVerry and Mauri McSaveney for their in-house reviews, and Matt Gerstenberger for his external review. Statistics New Zealand provided statistics on residential population of Westland localities.

REFERENCES

Cousins J., Spence, R. and So, E. (2008), "Estimated casualties in New Zealand earthquakes". *Proceedings Australian Earthquake Engineering Conference*, AAES 2008, November 21-23, Ballarat, Victoria, Australia.

Davenport, P.N. (2003), "Instrumental measures of earthquake intensity in New Zealand". *Pacific Conference on Earthquake Engineering*, Christchurch.

Dowrick, D.J. (1994), "Damage and intensities in the magnitude 7.8 1929 Murchison, New Zealand, earthquake". *Bulletin of the New Zealand National Society for Earthquake Engineering* **27**(3): 190-204.

Dowrick, D.J. and Rhoades, D.A. (1993), "Damage costs for commercial and industrial property as a function of intensity in the 1987 Edgecumbe earthquake". *Earthquake Engineering and Structural Dynamics* **22**: 869-884.

Dowrick, D.J. and Rhoades, D.A. (1999), "Attenuation of Modified Mercalli intensity in New Zealand earthquakes". *Bulletin of the New Zealand National Society for Earthquake Engineering* **32**(2): 22-89.

Dowrick, D.J. and Rhoades, D.A. (2005a), "Revised models for attenuation of Modified Mercalli intensity in New Zealand earthquakes". *Bulletin of the New Zealand Society for Earthquake Engineering* **38**(4): 185-214.

Dowrick, D.J. and Rhoades, D.A. (2005b), "Risk of casualties in New Zealand earthquakes". *Bulletin of the New Zealand Society for Earthquake Engineering* **38**(2): 53-72.

Dowrick, D.J. and Rhoades, D.A. (2010), "A distributed-source approach to modelling the spatial distribution of MM intensities resulting from large crustal New Zealand earthquakes". *Bulletin of the New Zealand Society for Earthquake Engineering* **43**(2): 85-109.

Dowrick, D.J., Rhoades, D.A. and Davenport, P.N. (2003), "Damage ratios for domestic property in the magnitude 7.2 1968 Inangahua, New Zealand, earthquake". *Bulletin*

of the New Zealand Society for Earthquake Engineering **36**(1): 25-46.

Dowrick, D.J., Hancox, G.T., Perrin, N.D. and Dellow, G.D. (2008), "The Modified Mercalli intensity scale: Revisions arising from New Zealand experience". *Bulletin of the New Zealand Society for Earthquake Engineering* **41**(3): 193-205.

McVerry, G.H., Zhao, J.X., Abrahamson, N.A., and Somerville, P.G. (2006), "New Zealand acceleration response spectrum attenuation relations for crustal and subduction zone earthquakes". *Bulletin of the New Zealand Society for Earthquake Engineering* **39**(1): 1-58.

NZS 1170.5 (2004), *Structural Design Actions Part 5: Earthquake Actions.* Standards New Zealand, Wellington.

Smith, W.D. (2002), "A model for MM intensities near large earthquakes". *Bulletin of the New Zealand Society for Earthquake Engineering* **35**(2): 96-107.

Somerville, P.G., Irakura, K., Graves, R., Sawada, S., Wald, D., Abrahamson, N., Iwasaki, Y., Kagawa, T., Smith, N. and Kowada, A. (1999), "Characterizing earthquake slip models for the prediction of strong ground motion". *Seismological Research Letters* **70**: 59-80.

Stirling, M.W.: Earthquake Hazards Team (2007), "Updating the national seismic hazard model for New Zealand". Paper 072, *Proceedings of the 8th Pacific Conference on Earthquake Engineering*, Singapore.

Sutherland, R. and 18 others (2007), "Do great earthquakes occur on the Alpine Fault in Central South Island, New Zealand?" In: *A Continental Plate Boundary: Tectonics at South Island, New Zealand. Geophysical Monograph Series No 175*: 235-251.